Templated Photocatalytic Synthesis of Well-Defined Platinum Hollow Nanostructures with Enhanced Catalytic Performance for Methanol Oxidation

Feng Bai,[†,‡] Zaicheng Sun,[‡,§] Huimeng Wu,[∥] Raid E. Haddad,[‡] Xiaoyin Xiao,[∥] and Hongyou Fan*[,‡,∥]

[†]Key Laboratory for Special Functional Materials of the Ministry of Education, Henan University, Kaifeng 475004, People's Republic of China

[‡]The University of New Mexico/NSF Center for Micro-Engineered Materials, Department of Chemical and Nuclear Engineering, Albuquerque, New Mexico 87131, United States

[§]Key Laboratory of Excited State Processes, Changchun Institute of Optics, Fine Mechanics and Physics, Chinese Academy of Sciences, 3888 East Nanhu Road, Changchun 130033, China

[∥]Sandia National Laboratories, Advanced Materials Laboratory, 1001 University Boulevard SE, Albuquerque, New Mexico 87106, United States

S *Supporting Information*

ABSTRACT: Hollow metallic nanostructures exhibit important applications in catalysis, sensing, and phototherapy due to their increased surface areas, reduced densities, and unique optical and electronic features. Here we report a facile photocatalytic process to synthesize and tune hollow platinum (Pt) nanostructures. Through hierarchically structured templates, well-defined hollow Pt nanostructures are achieved. These nanostructures possess interconnected nanoporous framework as shell with high surface area for enhanced catalytic performance/mass transport for methanol oxidation.

KEYWORDS: Self-assembly, photocatalytic reaction, methanol oxidation, platinum hollow nanostructure, fuel cell, porphyrin
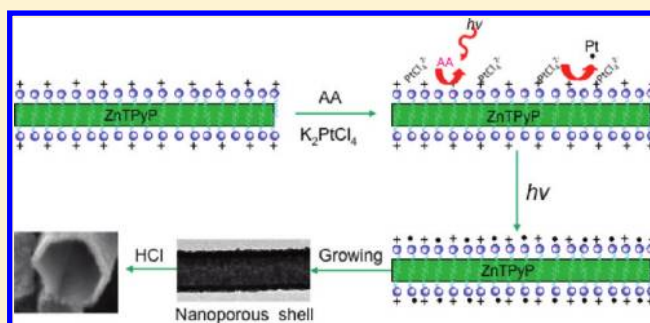
Hierarchically structured porous metallic nanostructures have received extensive research attention in recent years due to their increased surface areas, reduced densities, and unique optical and electronic features that lead to a broad range of important applications in catalysis, sensing, optical imaging, and phototherapy.[1−7] Ability to control the intrinsic nanostructure and morphology of these materials for tunable properties is essential for enhanced applications, yet technical challenges remain and have stimulated a wide range of synthesis efforts. Template synthetic methods have been established to be one of the convenient and effective methods to synthesize hollow nanostructures.[3,8−10] With these methods, either inorganic or organic particles are used as the sacrificial templates. Surface treatment is often required to form functional coating on the templates, in which case a complete coverage of functional coatings/groups on the template surface is important in order to achieve continuous and stable shells that do not collapse after removal of templates. Through template methods, both inorganic and polymer hollow particles have been prepared. In an extended method, a galvanic replacement reaction has been used to fabricate metallic hollow or core/shell nanostructures. In this method, the templates (e.g., Ag nanostructures) are synthesized first, and then converted via galvanic replacement reactions to another metal with complementary morphology beyond spherical particles.[5,11]
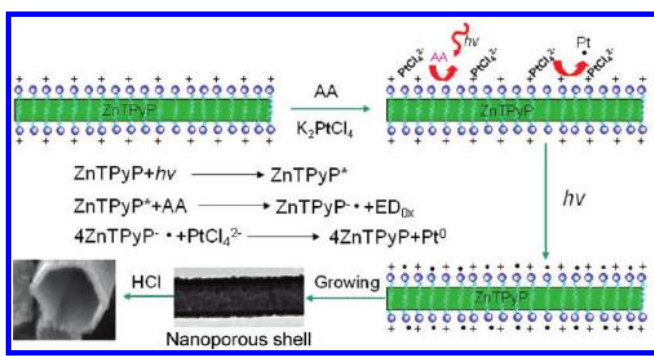
Continuing along the line to manipulate morphogenesis of hollow nanostructures, here we report a facile photocatalytic process to synthesize and tune Pt hollow nanostructures. We synthesized hierarchically structured porphyrin nanostructures and use them as both physical and chemical templates. At the molecular level, porphyrins possess unique photocatalytic properties, serving as a chemical template. On the nanoscale, controlled noncovalent assembly of porphyrins enables formation of ordered nanostructures with well-defined size and shape, providing a continuous physical template. The resultant Pt hollow materials have well-defined nanostructures that derive from the porphyrin templates and high accessible surface area, leading to enhanced active surface area for hydrogen adsorption and improved eletrocatalytic activity for methanol oxidation.

As shown in Scheme 1, we first synthesized well-defined optically active porphyrin nanostructures. Porphyrins are relatives

Scheme 1. Templated Photocatalytic Synthesis of Hollow Pt Nanostructures
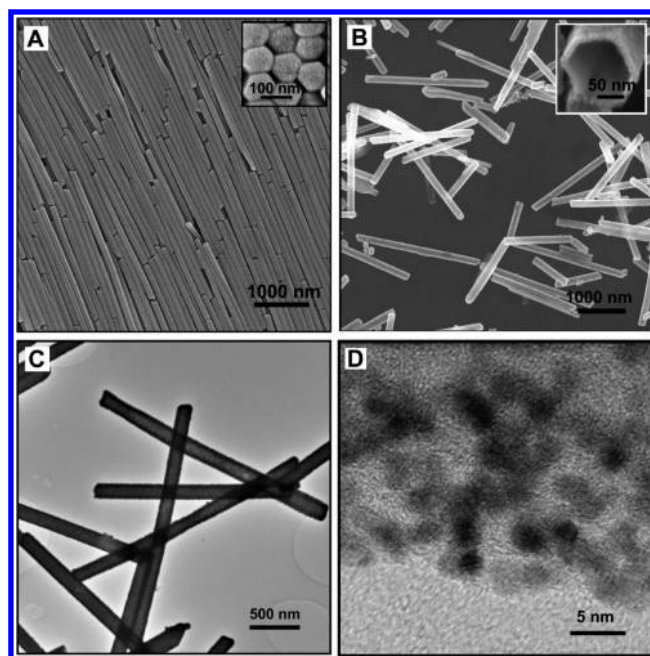

Figure 1. Electron microscopy images of the ZnTPyP long wires and the hollow Pt nanotubes. (A) SEM image of ZnTPyP long wires that have hexagonal shape for cross-sectional view. (B) SEM images of Pt nanotubes; inset, high-resolution SEM image shows the hexagonal shape of nanotube. (C) TEM image of Pt nanotubes. (D) Corresponding high-resolution TEM image shows the interconnected Pt network.

of biomolecules that exhibit essential optical and photocatalytic properties; for example, chlorophyll is one of the key elements in photosynthesis that absorbs light and conducts energy or charge transfer through redox processes inside green plants or bacteria.[12,13] Zinc *meso*-tetra(4-pyridyl)porphyrin (ZnTPyP) was chosen because, in addition to its favorable redox potentials for synthesis of Pt, it can self-assemble into ordered functional nanostructures that mimic photosynthetic systems in chloroplasts for enhanced electronic, optical, and photocatalytic functionality.[14] In general, these porphyrins self-organize through molecular noncovalent interactions such as metal−ligand coordination, $\pi-\pi$ stacking, hydrogen bonding, etc. The porphyrin nanostructures in this work were synthesized using a modified confined self-assembly method we developed recently.[14] Briefly, ZnTPyP is hydrophobic, so to make it soluble in water we added it into an acidic aqueous solution (e.g., aqueous HCl with pH 2) to protonate the pyridyl groups and form a tetrapyridinium cation ZnTPyPH^{4+}. We then added this ZnTPyPH^{4+} acidic aqueous solution to a basic aqueous solution of cationic surfactant (cetyltrimethylammonium bromide, CTAB) under stirring.

Acid−base neutralization reactions deprotonate the pyridinium cations, producing neutral ZnTPyPs that are insoluble in water. As they are deprotonated, the resultant hydrophobic ZnTPyPs are then sequestered within the hydrophobic micellar interiors.[15,16] Further self-assembly driven by intermolecular interactions such as metal−ligand axial coordination (Zn−N) and $\pi-\pi$ interactions initiates nucleation and growth of ZnTPyP crystalline nanostructures that are confined within surfactant micelles. As a result of the preparation process, the surfaces of the porphyrin nanostructures were deposited a thin layer of CTAB surfactants with positive charges (Scheme 1). Taking advantage of these positive charges, we then introduce metal precursor PtCl$_4^{2-}$ onto the porphyrin nanostructure surface through electrostatic interactions between the positively charged surface and negatively charged precursor. The photocatalytic reduction of platinum salts by the ZnTPyPs was conducted under visible light in the presence of an electron donor (ED), ascorbic acid (AA). The ZnTPyPs photoreaction is a reductive photocatalytic cycle. Through the photocatalytic reaction, K$_2$PtCl$_4$, is initially reduced to form highly uniform Pt nanoparticle seeds in the presence of light.[10,17] Then a shell of Pt nanoparticle networks is formed at the surface of the photoactive porphyrin nanostructures as Pt precursors are continuously reduced.

In a typical procedure for the synthesis of hollow Pt nanostructures (see details in Supporting Information), K$_2$PtCl$_4$ stock solution 0.5 mL (10 mM) and ascorbic acid stock solution

0.5 mL (0.1 M) were added to a 20 mL glass vial containing 10 mL of the ZnTPyP nanostructures with a concentration of 0.1 mg/mL. The reaction mixture was sonicated to homogenize the solution, and then irradiated with incandescent light (800 nmol cm^{-2} s^{-1}) for 30 min.[18,19] The reaction solution initially appears purple in color under incandescent light due to light scattering by the porphyrin nanostructures. As the photocatalytic reaction proceeds, the reaction solution turns black, suggesting that Pt^0 is formed. Through centrifugation, we collect the final black nanostructured Pt/porphyrin composite materials. To remove the porphyrin nanostructure templates, we disperse these Pt/porphyrin composite materials in HCl aqueous solution (1 N). As mentioned above, the acid protonates the four pyridyl groups of ZnTPyP to form a tetrapyridinium cation ZnTPyPH^{4+} that dissolves in the aqueous phase. After the ZnTPyP templates disolved, the hollow Pt nanostructures were collected by centrifugation.

The morphology of the hollow nanostructures is essentially determined by the shape of the initial ZnTPyP nanostructures. A variety of well-defined hollow structures can thus be fabricated by using templates of different shapes. We present first hollow Pt nanotubes (Figure 1) that were synthesized using hexagonal ZnTPyP nanowires as the templates. After removal of the ZnTPyP templates (Figure 1A), the Pt shells remain uncollapsed as hollow hexagonal nanotubes (Figure 1B inset), which suggests the mechanical stability of the hollow structures. The TEM images (Figure 1C) show that the Pt nanotubes have a uniform shell thickness of 15 ± 2 nm. The length of the nanotubes ranges from 2.3 to 2.6 μm, consistent with that of the initial templates, suggesting full coverage of Pt on the templates. High-resolution TEM images (Figure 1D) further reveal that the walls of the nanostructures are comprised of densely packed Pt nanoparticles.
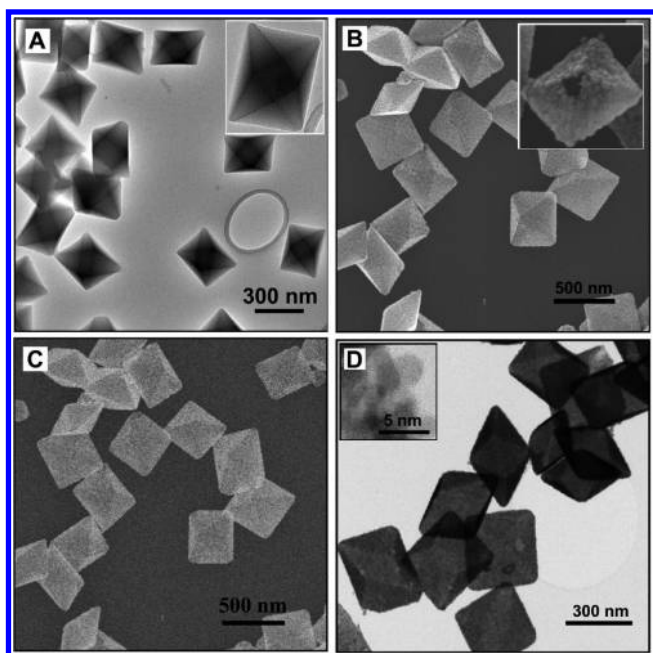
Figure 2. (A) TEM image of octahedral ZnTPyP nanocrystals. (B) SEM images of hollow Pt octahedrons; inset, high-resolution SEM image of one chipped specimen showing the hollow cavity. (C) Corresponding backscattering SEM image. (D) TEM image of hollow Pt octahedrons; inset, high-resolution TEM image shows the interconnected Pt particle network.

These Pt nanoparticles have an average size of 3.2 nm and form 3D interconnected Pt networks as shown by high-resolution TEM (Figure 1D). Detailed kinetic experiments indicate that both reaction time and concentration of the Pt precursor control the formation of Pt network within the shell. At about 5 min of reaction, fully self-supported nanotubes start to form; at concentration of 0.2 mM K_2PCl_4, nanotubes are formed (Figure S1, Supporting Information). Controlled experiments were also performed without light irradiation. In the absence of light, reduction of platinum salts by ascorbic acid occurred within minutes and resulted in macroscopic pieces of platinum metal that settled out of the solution rather than nicely coating the surface of ZnTPyP nanostructures.

The X-ray diffraction (XRD) patterns of the hollow nanostructures correspond to a face centered cubic crystal structure of metallic Pt (Figure S2A, Supporting Information). The relatively broad XRD lines suggest that the hollow shell is comprised of small Pt particles, consistent with TEM observations. It is noted that the diffraction patterns of porphyrin crystal were not detected within the XRD patterns of the hollow Pt structures, demonstrating that the porphyrin templates were completely removed after acidic solution washing.

In addition to the nanotubes, hollow Pt nanostructures with octahedral shape were successfully fabricated by using octahedral porphyrin crystals as templates. Figure 2 shows that Pt nanoparticles grow and deposit on the surface of octahedral porphyrin nanostructures. The octahedral shape is conserved after removal of the templates (Figure 2B−D) without collapse. XRD patterns confirmed the complete removal of the templates (Figure S2B, Supporting Information). It is thus suggested that the Pt nanoparticles are interconnected to form a stable shell. The backscattering SEM image of the hollow octahedrons (Figure 2C)
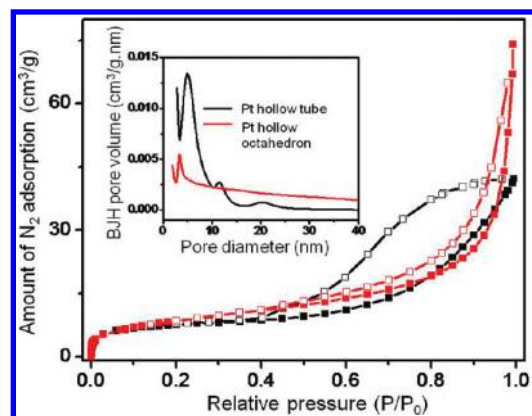

Figure 3. Nitrogen sorption isotherms obtained at 77 K for different hollow Pt nanostructures: nanotube (diameter ∼150 nm, thickness 15 nm), octahedron (diameter 280 nm, thickness 10 nm): adsorption, solid data markers; desorption, open data markers; inset, pore size distributions for different Pt hollow nanostructures.

indicates Pt nanoparticles are uniformly distributed within the shell. High-resolution TEM images (Figure 2D, inset) further show that the submicrometer Pt octahedrons consist of interconnected Pt nanoparticles with size ranging from 3.5 to 4.2 nm.

Due to the interconnected 3D network formed, these hollow Pt nanostructures are nanoporous and have very high surface area. Nitrogen sorption was performed to characterize the porosity of different hollow Pt nanostructures, and the nitrogen isotherms are shown in Figure 3. Overall, the Pt frameworks exhibit major mesoporous structure (∼5.5 nm) with some macropores. Table S1 in the Supporting Information summarizes the pore size, porosity, and surface area of these Pt nanostructures.

We studied hydrogen adsorption and methanol oxidation on these well-defined Pt nanostructures. Figure 4A shows the cyclic voltammograms of Pt octahedrons compared to a commercial catalyst made of Pt nanoparticles on carbon support (purchased from Alfa Aesar, 40 wt % Pt, TEM image shown in Figure S3 in the Supporting Information). Both catalysts show the comparable and pronounced hydrogen adsorption peaks at ∼0.10 and 0.23 V, indicating high density of the {110} facets of Pt nanoparticles. Pt octahedrons show relatively smaller capacitive charges. The integrated hydrogen adsorption charges between 0 and 0.37 V are about 1.93 and 2.38 mC, which correspond to electrochemical active surface areas of 32 m^2/g for the Pt octahedrons and 44 m^2/g for the commercial catalyst assembled at the same glass carbon electrode. We calculate the active surface areas using 0.21 mC/cm^2 as a reference value often used for a monolayer of hydrogen adsorption at Pt polycrystalline electrode.[1,20] Figure 4B shows their electrocatalytic activities for methanol oxidation. Remarkably, the Pt octahedrons demonstrate much enhanced methanol oxidation activity. First, the oxidation potential is shifted about 35 mV to the negative direction; second, the current density is increased from 0.418 to 0.688 mA/cm^2, about 65% of increase in the forward positive scan and 30% of increase in the backward negative scan; third, the ratio of peak current in the positive scan versus the backward negative scan is 0.75, which is much greater than that from the commercial catalyst (∼0.58). The larger this ratio is, the better the catalyst's CO tolerance.[21,22] The enhanced methanol oxidation and high CO tolerance result from small Pt nanoparticles densely integrated into porous nanostructured networks. The pores within the nanostructures are
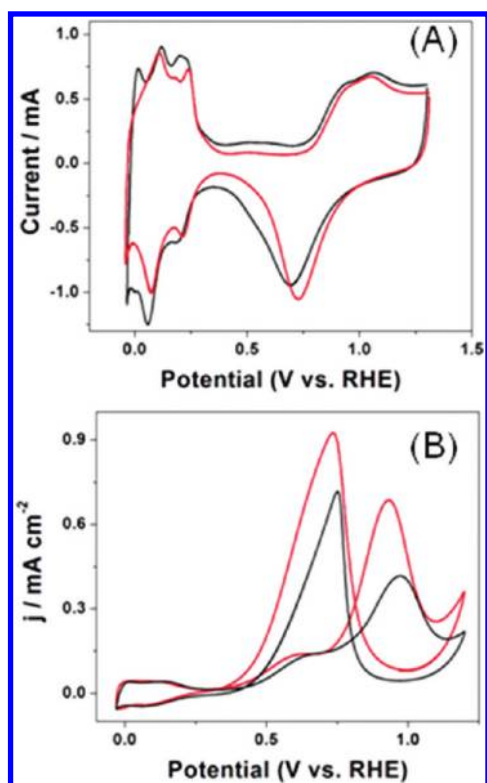
Figure 4. Cyclic voltammograms of Pt octahedrons (red) and commercial Pt/C (black) in 0.5 M H_2SO_4 (A) and 0.5 M H_2SO_4 + 0.5 M MeOH (B). Scan rate: 100 mV/s.

large enough that they may also improve mass transport of methanol through the Pt shell.

In summary, we developed a templated photocatalytic approach for the synthesis of well-defined Pt hollow nanostructures that have enhanced catalytic performance/mass transport for methanol oxidation. The approach is simple, clean, and economic. The templates contain densely packed optically active porphyrins, leading to continuous templating of Pt seeds and growth of networks under light irradiation. Because of the fact that ZnTPyP templates can be dissolved through an acid–base neutralization process, the ZnTPyP can be recycled and reused for continuous fabrication of hollow Pt nanostructures. We anticipate synthesizing other metal hollow nanostructures or metal alloys by using different types of porphyrinic nanocrystalline templates. Ongoing efforts now focus on the fabrication of hierarchical structures such as hexagonal honeycomb structures by using self-assembled ZnTPyP nanostructure arrays.

■ ASSOCIATED CONTENT

ⓢ Supporting Information. Experimental details, figures showing TEM images, and table of pore size and surface areas for the Pt hollow nanostructures. This material is available free of charge via the Internet at http://pubs.acs.org.

■ AUTHOR INFORMATION

Corresponding Author
*E-mail: hfan@sandia.gov.

■ REFERENCES

(1) Chen, A.; Holt-Hindle, P. *Chem. Rev.* **2010**, *110* (6), 3767–3804.
(2) Kim, S.-W.; Kim, M.; Lee, W. Y.; Hyeon, T. *J. Am. Chem. Soc.* **2002**, *124* (26), 7642–7643.
(3) Liang, H.-P.; Zhang, H.-M.; Hu, J.-S.; Guo, Y.-G.; Wan, L.-J.; Bai, C.-L. *Angew. Chem., Int. Ed.* **2004**, *43* (12), 1540–1543.
(4) Mazumder, V.; Lee, Y.; Sun, S. *Adv. Funct. Mater.* **2010**, *20* (8), 1224–1231.
(5) Sun, Y.; Mayers, B.; Xia, Y. *Adv. Mater.* **2003**, *15* (7–8), 641–646.
(6) Zhang, Q.; Wang, W.; Goebl, J.; Yin, Y. *Nano Today* **2009**, *4* (6), 494–507.
(7) Kawasaki, J. K.; Arnold, C. B. *Nano Lett.* **2011**, *11* (2), 781–785.
(8) Braun, P. V.; Osenar, P.; Stupp, S. I. *Nature* **1996**, No. 380, 325–328.
(9) Braun, P. V.; Osenar, P.; Tohver, V.; Kennedy, S. B.; Stupp, S. I. *J. Am. Chem. Soc.* **1999**, *121* (32), 7302–7309.
(10) Song, Y.; Yang, Y.; Medforth, C. J.; Pereira, E.; Singh, A. K.; Xu, H.; Jiang, Y.; Brinker, C. J.; van Swol, F.; Shelnutt, J. A. *J. Am. Chem. Soc.* **2003**, *126* (2), 635–645.
(11) Mayers, B.; Jiang, X.; Sunderland, D.; Cattle, B.; Xia, Y. *J. Am. Chem. Soc.* **2003**, *125* (44), 13364–13365.
(12) Blankenship, R. E., *Molecular Mechanisms of Photosynthesis*; Blackwell: Oxford, 2002.
(13) Mauzerall, D. C. *Clin. Dermatol.* **1998**, *16* (2), 195–201.
(14) Bai, F.; Wu, H.; Haddad, R. E.; Sun, Z.; Schmitt, S. K.; Skocypec, V. R.; Fan, H. *Chem. Commun.* **2010**, *46* (27), 4941–4943.
(15) Fan, H.; Yang, K.; Boye, D. M.; Sigmon, T.; Malloy, K. J.; Xu, H.; Lopez, G. P.; Brinker, C. J. *Science* **2004**, *304* (5670), 567–571.
(16) Barber, D. C.; Freitag-Beeston, R. A.; Whitten, D. G. *J. Phys. Chem.* **2002**, *95* (10), 4074–4086.
(17) Song, Y.; Garcia, R. M.; Dorin, R. M.; Wang, H.; Qiu, Y.; Shelnutt, J. A. *Angew. Chem., Int. Ed.* **2006**, *45* (48), 8126–8130.
(18) Song, Y.; Garcia, R. M.; Dorin, R. M.; Wang, H.; Qiu, Y.; Coker, E. N.; Steen, W. A.; Miller, J. E.; Shelnutt, J. A. *Nano Lett.* **2007**, *7* (12), 3650–3655.
(19) Wang, H.; Song, Y.; Medforth, C. J.; Shelnutt, J. A. *J. Am. Chem. Soc.* **2006**, *128* (29), 9284–9285.
(20) Campbell, D. J.; Corn, R. M. *J. Phys. Chem.* **1988**, *92* (20), 5796–5800.
(21) Gasteiger, H. A.; Markovic, N.; Ross, P. N.; Cairns, E. J. *J. Phys. Chem.* **1993**, *97* (46), 12020–12029.
(22) Wang, H.; Löffler, T.; Baltruschat, H. *J. Appl. Electrochem.* **2001**, *31* (7), 759–765.